

# Local bond-slip behavior of medium and high strength fiber reinforced concrete after exposure to high temperatures

Chao-Wei Tang\*

Department of Civil Engineering & Geomatics, Cheng Shiu University, No. 840, Chengcing Rd.,  
Niasong District, Kaohsiung City, Taiwan R.O.C.

(Received December 15, 2017, Revised February 23, 2018, Accepted February 27, 2018)

**Abstract.** This study aims to investigate the influence of individual and hybrid fiber on the local bond-slip behavior of medium and high strength concrete after exposure to different high temperatures. Tests were conducted on local pullout specimens (150 mm cubes) with a reinforcing bar embedded in the center section. The embedment lengths in the pullout specimens were three times the bar diameter. The parameters investigated include concrete type (control group: ordinary concrete; experimental group: fiber concrete), concrete strength, fiber type and targeted temperature. The test results showed that the ultimate bond stress in the local bond stress versus slip curve of the high strength fiber reinforced concrete was higher than that of the medium strength fiber reinforced concrete. In addition, the use of hybrid combinations of steel fiber and polypropylene fiber can enhance the residual bond strength ratio of high strength concrete.

**Keywords:** hybrid fiber reinforced concrete; residual bond strength; pullout test

## 1. Introduction

Reinforced concrete (RC) is by far one of the most widely used construction material in the world. In general, the performance of RC structures depends mainly on sufficient bond strength between reinforcing steel and surrounding concrete (ACI Committee 408 2003, Golafshani *et al.* 2012, Alexandre *et al.* 2014, Deng *et al.* 2014, Golafshani *et al.* 2014a, Golafshani *et al.* 2014b, Dehestani and Mousavi 2015, Golafshani *et al.* 2015, Mo *et al.* 2015, Tang 2015, Choi and Lee 2015, Zhang and Yu 2016, Tang 2017). According to the ACI 318 (ACI Committee 318 2014), bond stress is a shear stress transmitted along the interface between reinforcing steel and surrounding concrete. Basically, the bond behavior between rebar and surrounding concrete is mostly composed of three resistance mechanisms: adhesion, friction resistance, and rib support. Among them, rib support is the most important mechanism. However, the bond performance in RC structures under elevated temperatures will gradually decline owing to incompatible dimensional changes between cement paste and aggregate. As a result, the structural performance of RC structures will be seriously affected.

Based on compressive strength, concrete can be classified into four broad categories: low strength concrete (less than 20 MPa), moderate strength concrete (20 to 40 MPa), high strength concrete (more than 40 MPa), and ultra high strength concrete (more than 150 MPa). However, the bottom range of strength of various concrete varies with time and geographical location. In the North American

practice (ACI 318 1999), high strength concretes (HSCs) are those that attain cylinder compressive strength of at least 41 MPa at 28 days. While, in the FIP/CIB (1990) state-of-the-art report on high strength concrete, it is defined as concrete having a 28-day cylinder compressive strength of 60 MPa. In the study, medium strength concrete is tentatively defined as the concrete having the strength of 40-60 MPa, while HSC is defined as the concrete having the strength of more than 60 MPa. HSC has many advantages, which have been widely used in various construction projects. For instance, the use of HSC can reduce size and reinforcement in structural members, such as columns, and increase useable space, especially in high-rise buildings.

High temperature will cause the volume change of concrete, which is the sum of the changes in volume of cement paste and aggregate. In particular, HSC exposed to an abrupt temperature rise is more likely to lead to explosive spalling, which refers to a sudden and violent breaking away of a surface layer of heated concrete. The spalling is caused by the thermal stress due to the temperature gradient during heating (Ko *et al.* 2011). In view of this, there are many studies to explore the spalling behavior of HSC subjected to elevated temperatures. For instance, the use of fiber reinforced concrete (FRC) is a viable option (Mehta and Monteiro 2006). Compared with ordinary concrete, FRC has better toughness and impact resistance (Xiong and Richard Liew 2015, Xu *et al.* 2016, Kim *et al.* 2016, Lee and Yi 2016, Kim *et al.* 2017, Nematzadeh and Poorhosein 2017, Saleem 2017). Varona *et al.* (2018) investigated the influence of high temperature on the mechanical properties of hybrid fiber reinforced normal and high strength concrete. Their test results showed that the effect of high temperature on the residual mechanical properties of hybrid fiber reinforced concretes was less

\*Corresponding author, Professor  
E-mail: [tangcw@gcloud.csu.edu.tw](mailto:tangcw@gcloud.csu.edu.tw)

severe than in steel fiber reinforced concretes found in previous references. On the other hand, it was observed that polypropylene fibers can mitigate or prevent the explosive spalling (Poon *et al.* 2004, Siddique and Kaur 2012, Ding *et al.* 2012, Ozawa and Morimoto 2014, Yan *et al.* 2015). This is because the polypropylene fibers melt after the temperature inside concrete reaches approximately 170°C, which produces micro channels for release of vapor pressure of concrete; and thus, the amount of heat absorbed is less for dehydration of chemically bound water (Bilodeau *et al.* 2004, Kodur 2014, Xiong and Richard Liew 2015). However, at different temperatures, the effect of polypropylene fiber on compressive strength and flexural strength of HSC with different strength levels is very different, that is, its recovery strength is questioned (Chan *et al.* 2000, Poon *et al.* 2004).

In view of the above considerations, the microstructure and mechanical properties of concrete under elevated temperatures may significantly deteriorate and thus affect the bond performance in RC structures. The review of literature indicates that limited research has been undertaken to investigate the role of fibers in maintaining post-heating bond between concrete and steel rebar (Ergün *et al.* 2016, Ruano *et al.* 2018). Therefore, this study aimed at conducting an investigation on the local bond-slip behavior of various fiber-reinforced concretes after exposure to different high temperatures.

## 2. Experimental procedure

### 2.1 Experimental program

In this study, local pullout tests with a concentric reinforcing bar in concrete were adopted for experimental determination of the local bond-slip relationship between rebar and concrete. Local pullout tests were conducted on 150×150×150 mm concrete cube specimens with only a fraction of their length in contact with confined concrete. The specimens were divided into two groups to investigate the effect of adding different amounts of fiber on their residual bond strength and bond strength-slip response after exposure to temperature levels of 400, 600, and 800°C in addition to the room temperature. The test parameters analyzed were concrete type (control group: ordinary concrete; experimental group: fiber concrete), concrete strength, fiber type, and targeted temperature. The variables for test are shown in Table 1.

Table 1 Planning of experimental variables

Group	Mix No.	Specified concrete strength	Fiber content (Volume %)	Targeted temperature (°C)
Control group	N45	45 MPa	0	400, 600, and 800
	N75	75 MPa	0	400, 600, and 800
Experimental group	F45-S	45 MPa	Steel fiber (1%)	400, 600, and 800
	F75-S	75 MPa	Steel fiber (1%)	400, 600, and 800
	F75-P	75 MPa	Polypropylene fiber (0.1%)	400, 600, and 800
	F75-M	75 MPa	Steel fiber (1%) + Polypropylene fiber (0.1%)	400, 600, and 800

Table 2 Physical properties of coarse/fine aggregate

Aggregate type	Specific weight (SSD)	Water absorption (SSD) (%)	Unit weight (dry-rodged) (kg/m <sup>3</sup> )	FM
Coarse aggregate	2.63	1.17	1532	-
Fine aggregate	2.60	1.25	-	2.70

Notes: SSD=saturated surface dry condition; FM=fineness modulus

Table 3 Physical and mechanical of deformed bar

Bar No.	Nominal dia. (mm)	Nominal cross section area (cm <sup>2</sup> )	Rib distance (mm)	Rib width (mm)	Rib height (mm)	Yield strength (N/mm <sup>2</sup> )
3	9.53	0.71	6.1	3.4	0.5	468.3
6	19.12	2.87	12.3	4.5	1.5	489.5

### 2.2 Materials and mix proportions

Materials used for making specimens included cement, slag, fine and coarse aggregates, fiber, superplasticizer, and reinforcing bar. Local ordinary Portland cement (OPC) with a specific gravity of 3.15 and a fineness of 3400 cm<sup>2</sup>/g complying with ASTM C150/C150M (ASTM C150/C150M-15 2015) was used. Local slag with a specific gravity of 2.9 and a fineness of 6000 cm<sup>2</sup>/g was used. Well-graded aggregate and washed natural sand were selected in accordance with ASTM C33/C33M (ASTM C33/C33M-13 2013). The coarse aggregate was crushed stone with a maximum particle size of 19 mm, and the fine aggregate was natural river sand. The physical properties of these aggregates are shown in Table 2. Local steel fibers and polypropylene fibers were used. Sikament-1250 produced by Sika Taiwan Ltd. was used as a superplasticizer in the production of concrete. To ensure the rheological and mechanical properties of the fiber reinforced concrete, the fiber content used was 0.1% (volume fraction). This amount of fiber can avoid the problem of mixture workability associated with the addition of PP fibers (balling and clumping of fibers). At the same time, the fracture modulus and fracture toughness of the fiber reinforced concrete can be properly increased. The reinforcing bars used included No. 3 and No. 6. The physical and mechanical properties of these reinforcing bars are shown in Table 3.

In this study, two types of concrete were prepared: fiber concrete (FC) and ordinary concrete (NC), the latter serving as the reference concrete. To analyze the influence of concrete strength on the bond behavior, the specified 28-day compressive strengths were chosen equal to 45 and 75 MPa for medium and high strength concrete, respectively. Some trial mixtures were prepared to obtain the target strength at 28 days, along with a proper workability of 90 to 200 mm. The mix proportions for the FC and the NC are given in Table 4. The abbreviations for identifying each concrete indicate the type of concrete –fiber concrete (F) or ordinary concrete (N), the strength of concrete (45 or 75 MPa), and the type of fiber (S: steel fiber, P: polypropylene fiber, M: hybrid fiber).

Prior to mixing, the aggregates were cured indoors until the required saturated surface-dry condition was reached. In mixing, the cement, slag, fiber, fine aggregates, and coarse

Table 4 Mix proportions of concrete

Group	Mix No.	W/B	Cement (kg/m <sup>3</sup> )	Slag (kg/m <sup>3</sup> )	Water (kg/m <sup>3</sup> )	Aggregate (kg/m <sup>3</sup> )		SP (kg/m <sup>3</sup> )	Steel fiber (kg/m <sup>3</sup> )	PP (kg/m <sup>3</sup> )
						FA	CA			
Control group	N45	0.50	270	90	180	775	1020	2.1	-	-
	N75	0.35	386	128	180	645	1020	3.375	-	-
Experimental group	F45-S	0.50	270	90	180	775	1020	2.1	78	0
	F75-S	0.36	386	112	180	645	1020	3.375	78	0
	F75-P	0.36	386	112	180	645	1020	3.375	0	0.9
	F75-M	0.36	386	112	180	645	1020	3.375	78	0.9

Note: F=fiber concrete; N=ordinary concrete; digits=strength level; W/B=water/binder ratio; FA=fine aggregate; CA=coarse aggregate; SP=superplasticizer; PP=polypropylene fiber

aggregates were generally blended first, and then water and superplasticizer were added. The mixing continued until a uniform concrete without any segregation was obtained.

### 2.3 Casting of specimens

The pullout specimens tested were cubes of 150×150×150 mm with a single No. 6 bar embedded vertically along the central axis (see Fig. 1). The embedment lengths ( $l_a$ ) in the pullout specimens were determined to be three times the bar diameter ( $d_b$ ), i.e.,  $l_a=3d_b$ . This anchorage length is short enough to assume that the bond stresses are evenly distributed in all loading stages. In other words, the slippage recorded is representative of a local bond stress value (Soroushian *et al.* 1994). Those unbounded regions of the bar were sheathed with a PVC pipe. In addition, three lateral stirrups (No. 3 rebar) were embedded in the test specimens to prevent the concrete from splitting when the reinforcing bar was in tension. Two nominally identical specimens were tested for each concrete mix to check the validity of the test setup and the variations in test results.

All the pullout specimens were cast in steel molds. Freshly mixed concrete was slowly poured into the pullout specimen mold and then was thoroughly compacted with a mechanical vibrator. On the other hand, six cylinder specimens of concrete (100 mm in diameter and 200 mm in height), referred to hereafter as control cylinders, were also cast with suitable external vibration for each mixture. After casting, all the specimens were covered with a wet hessian and polyethylene sheets overnight. The pullout specimens with their respective control cylinders were then demolded after 24 hours. Following demolding, all the specimens were immediately submerged in a water curing tank in the laboratory for 27 days. Testing was conducted at 28 days after casting.

### 2.4 Instrumentation and test procedures

The tests of compressive strength for concrete were performed according to ASTM C39 standard. The pullout tests were performed according to ASTM C234 standard. A 500 kN MTS servo controlled universal testing machine

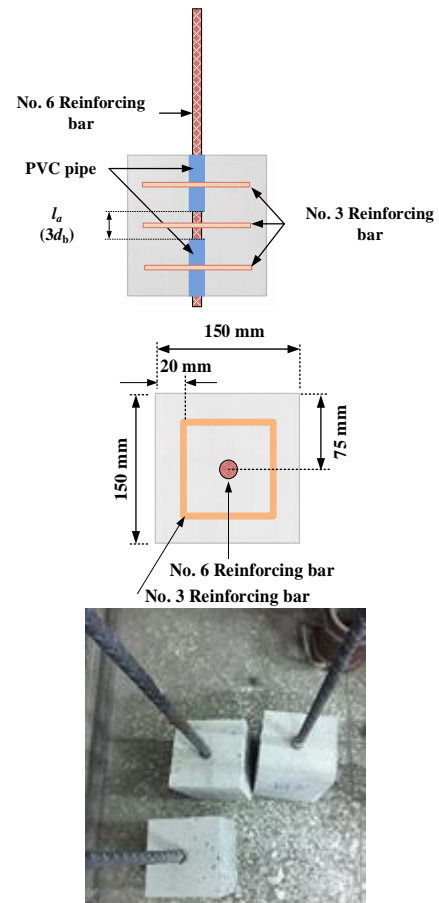


Fig. 1 Dimensions and cross-sections of test specimen

equipped with a specially fabricated testing frame was used (Fig. 2), which was capable of measuring the movement of the bar with respect to the concrete at both the loaded and free (unloaded) ends of the bar. Linear variable differential transformers (LVDTs) were used to measure the relative bond slip between bar and concrete at the loaded as well as the free ends; the detailed test setup is shown in Fig. 2. Both ends of the specimen were fixed on the bracket of the displacement device and the 6 mm-LVDT was installed. Then, the specimen was placed between the two steel plates and the tail end of the steel bar was fixed to the punch of the universal testing machine. Subsequently, the pullout force was applied at a constant displacement rate of 0.01 mm/sec up to bond failure (RILEM 1994). The pullout force was measured by a load cell fitted in the testing machine. The test progress was monitored on a computer screen, and all the load and displacement data were captured and stored in a diskette via a data logger.

On the other hands, the specimens were heated without preload at a prescribed rate (10°C/min.) until the temperature inside the furnace reached the target temperatures. After achieving the targeted maximum temperature, the furnace temperature was maintained for 60 minutes to achieve a thermal steady state in the whole specimen (Fig. 3). In other words, depending on the target temperature (400, 600 and 800°C), the specimens had different exposure times of 100, 120 and 140 minutes, respectively. The furnace power switch was then turned off,

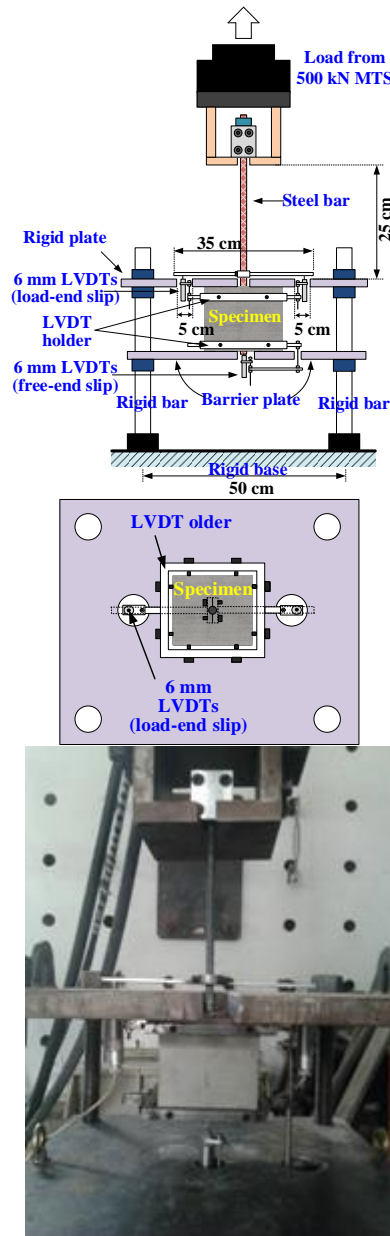


Fig. 2 Setup of pullout test

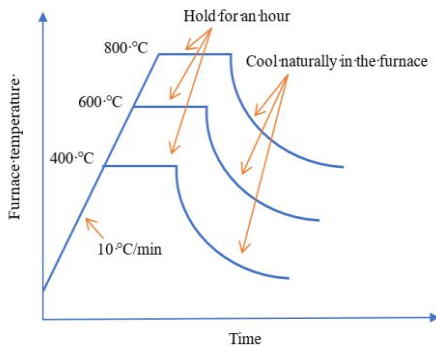


Fig. 3 Temperature versus time curve in the furnace for the pullout specimens

and the specimens were allowed to cool slowly in the furnace with the door opened. Upon cooling to room

Table 5 Results of slump, unit weight and compressive test of concrete

Group	Mix No.	Slump (cm)	Unit weight (kg/m <sup>3</sup> )	Compressive strength (MPa)
Control group	N45	18	2205	46.6
	N75	21	2259	80.0
Experimental group	F45-S	18	2284	49.6
	F75-S	20	2338	79.2
	F75-P	9	2270	75.0
	F75-M	9	2347	81.6

temperature, the residual bond strength tests were carried out.

### 3. Experimental results and discussion

#### 3.1 Fresh and mechanical properties of concrete

Fresh concrete properties were measured immediately after the mixing procedure. The results of slump and unit weight test of concrete in the control and experimental groups are shown in Table 5. As can be seen from Table 5, the slump value ranged from 9 to 21 cm. For the control group, the N45 mix had a slump of 18 cm, and the N75 mix had a slump of 21 cm owing to a high dosage of superplasticizer. That is to say, the concrete of the control group had a very good workability. As for the experimental group, the F75-S mix with steel fiber had a slump of 20 cm, but the slump of both the F75-P and F75-M mixes with polypropylene fiber was only 9 cm. The reason is that the polypropylene fibers are very fine (about 50000-300 million strands per kilogram), resulting in a stiffer mixture and leading to reduced workability. In addition, Table 5 shows that in the control group, the unit weights were 2205 and 2259 kg/m<sup>3</sup> for the N45 and N75 mixes, respectively. In other words, there was no significant difference in unit weight between the two mixes. For the experimental group, the unit weight of the F45-S, F75-S, and F75-M mixes with the addition of steel fiber was heavier (between 2284 and 2347 kg/m<sup>3</sup>), while the unit weight of the F75-P mix only with the addition of polypropylene fiber was lighter (2270 kg/m<sup>3</sup>).

At 28 days of age, the cylinders of each concrete mix were capped with gypsum capping compound and tested in compression to determine the compressive strength of concrete. Mean compressive strength was calculated by taking average of three specimens. As can be seen from Table 5, the compressive strength of both the control group and experimental group can be higher than the specified 28-day compressive strength at normal temperature. In addition, comparing the strength of concrete with medium strength (the N45 and F45-S mixes), it can be seen that the addition of steel fiber can improve its 28-day compressive strength. For high strength concrete (the N75, F75-S, and F75-M mixes), with the exception of the F75-P mix, the strength of the experimental group was larger than that of the control group.

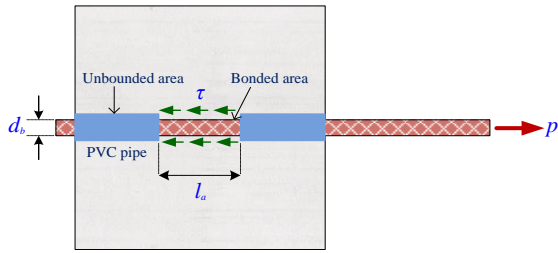


Fig. 4 Schematic diagram of local bond stress between bar and concrete

### 3.2 Local bond stress-slip relationship

During the loading of the pullout test, by measuring the relative slip of concrete and rebar as well as the corresponding force, the local bond stress versus slip curve from specimen loading to failure can be obtained. Assuming that the bond stresses are uniformly distributed along the bonded length (see Fig. 4), the bond stress can be obtained from the internal force balance of the specimen, as shown in the following equation

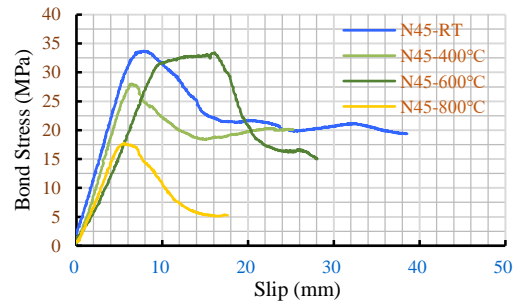
$$\tau = \frac{P}{\pi d_b l_a} \quad (1)$$

where  $\tau$  is the bond stress (MPa);  $P$  is the pullout force (N);  $d_b$  is the bar diameter (mm);  $l_a$  is the bond length (mm).

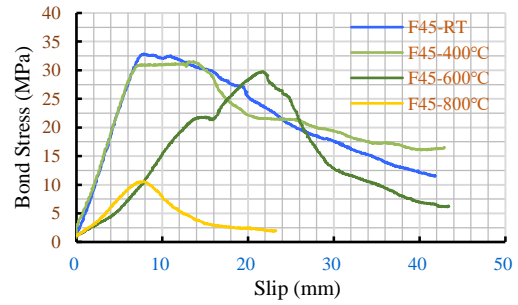
The relative slip between steel bar and concrete corresponding to the bond stress can be divided into the loading end slip  $s_l$  and the free end slip  $s_f$ . In the case of local bond, the relative slip of the steel and concrete can be regarded as rigid body motion, so the  $s_l$  and  $s_f$  should be the same under the same loading. In this study, the average of the two is the slip of the corresponding bond stress, as follows

$$s = (s_l + s_f)/2 \quad (2)$$

Using the Eqs. (1) and (2), the results of the pullout tests can be calculated. The details of the local bond stress versus slip curve are shown in Figs. 5-6. Overall, in the case of a steel bar embedded with a short length, a good stirrup confining effect and a sufficient thickness of the protective layer of the specimen, the pullout specimens were shear failure. In other words, the type of bond damage of the pullout specimens was pull-out failure. The complete behavior of the bond stress-slip relationship for the specimens was characterized by an initial increase in the bond stress with negligible slips because of the adhesion between bar and matrix. With the increasing load, the adhesion gradually declined. When the loading increased continuously and the bond stress reached splitting bond stress ( $\tau_{cr}$ ), radial splits appeared around the bar due to radial pressure exerted by the bar lugs. Afterwards, the relative slip occurred between bar and matrix, which was then followed by softening once the ultimate bond stress ( $\tau_u$ ) had been reached. Immediately, the bond stress decreased quickly and the slip increased sharply. As a result, only the friction between the bar and the surrounding concrete can be considered as the residual bond stress ( $\tau_r$ ) when the amount of slip reached about one to two times the



(a) Control group



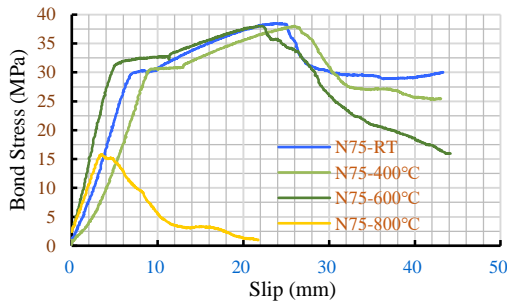
(b) Experimental group

Fig. 5 Local bond stress versus slip curve of medium strength concrete

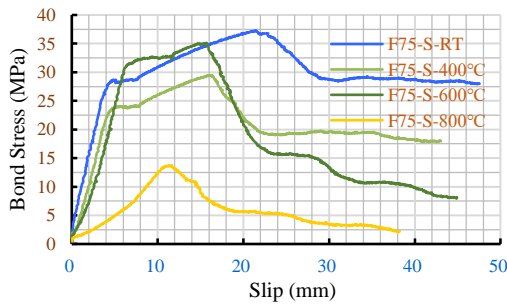
net spacing of ribs.

For the medium strength concrete, the relationship between bond stress and slip is shown in Fig. 5. It can be seen from Fig. 5 that at room temperature, the ultimate bond stress of the control group (the N45 mix) and the experimental group (the F45-S mix) demonstrated similar responses up to the peak value, but different energy dissipation in the post-peak branch. Overall, the incorporation of steel fibers could enhance the post-peak branch of the local bond stress versus slip curve. In addition, the ultimate bond stress of the N45 specimen was obviously attenuated when the temperature was 400°C, but the ultimate bond stress of the F45-S specimen was only slightly attenuated. The reason is mainly due to the drying effect of the sample at high temperature, and thus leading to increased strength (Siddique and Kaur 2012). Moreover, the evaporable water (capillary water, adsorbed water and interlayer water) can be removed because of the drying effect at high temperature, and the pore pressure formed by the high temperature can be reduced to increase the ultimate bond stress. On the other hand, at different temperatures, the slip of the N45 specimen in the control group of medium strength concrete was relatively small, which was about 5-16 mm. In contrast, the F45-S specimen had a relatively large amount of slip corresponding to the ultimate bond stress, which was about 7-22 mm.

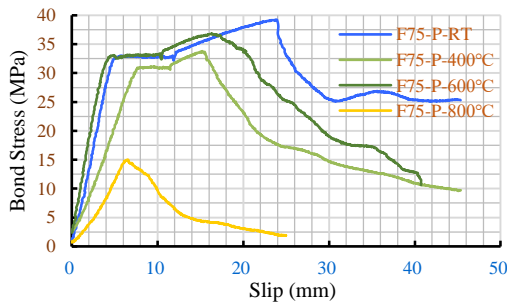
As for the high strength concrete, the local bond stress-slip curves are shown in Fig. 6. It is worth mentioning that, with the increase of concrete strength, the splitting bond stress ( $\tau_{cr}$ ) in the local bond stress versus slip curve of the high strength concrete was higher than that of the medium strength. It can be seen from Fig. 6 that at the temperature of 400°C, the ascending slope of the local bond stress



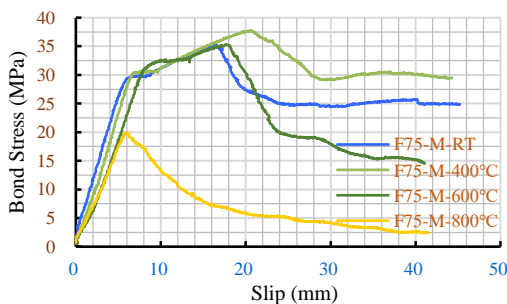
(a) Control group N75



(b) Experimental group F75-S



(c) Experimental group F75-P



(d) Experimental group F75-M

Fig. 6 Local bond stress versus slip curve of high strength concrete

versus slip curve of the control group (the N75 mix) specimen was obviously attenuated, while the ascending slope of the F75-S and F75-M specimens in the experimental group was only slightly attenuated. On the other hand, at different temperatures, the slip at the ultimate bond stress of the N75 specimen in the control group of high strength concrete was quite large (except 800°C), and its value was about 25-27 mm. In contrast, the slip of the experimental group at 800°C was relatively small, which was about 6-11 mm.

Table 6 Results of bond stress, residual bond stress and residual bond strength ratio

Group	Mix No.	Bond strength (MPa)	Residual bond strength (MPa)			Residual bond strength ratio		
		Room temperature	High temperature			High temperature		
			400°C	600°C	800°C	400°C	600°C	800°C
Control group	N45	28.9	24.0	28.7	15.2	0.83	0.99	0.53
	N75	33.0	32.6	32.6	13.6	0.99	0.99	0.41
Experimental group	F45-S	28.2	27.0	25.5	9.1	0.96	0.90	0.32
	F75-S	32.0	25.2	30.1	11.8	0.79	0.94	0.37
	F75-P	33.6	29.0	31.6	12.9	0.86	0.94	0.38
	F75-M	30.2	32.4	30.3	17.1	1.07	1.00	0.57

### 3.3 Ultimate bond stress

For RC members subjected to external forces, when the bond stress between the concrete and the reinforcement reaches the maximum allowable value, the members will lose their ability to resist external forces. In view of this, by comparing the ultimate bond stress of each specimen, it is possible to evaluate whether the bond strength of the sample is good or bad. In particular, in the case of the local pullout test, the influence of the uneven force distribution along the embedded length of the steel bar can be eliminated, and thus the comparison results are more representative. Table 6 presents the experimental results of ultimate bond stress for each specimen. It can be seen from Table 6 that the bond strength at 28 days of age in the control group and the experimental group can be higher than 28 MPa at room temperature. In addition, comparing the bond strength of moderate strength concrete (the N45 and F45-S mixes), it can be concluded that the incorporation of steel fiber did not help to improve its 28-day bond strength. On the other hand, for the 28-day bond strength of the high strength concrete, the value of the F75-P mix was greater than that of the N75 mix, but the values of the F75-S and F75-M mixes were smaller than that of the N75 mix.

Table 6 also lists the residual bond strength of each concrete mixture after being exposed to different high temperatures. In the control group, the residual bond strength of the N45 mix was between 15.2-28.7 MPa, while the residual bond strength of the N75 mix was between 13.6-32.6 MPa. In the experimental group, the residual bond strength ranged from 9.1 to 27.0 MPa, from 11.8 to 30.1 MPa, from 12.9 to 31.6 MPa, and from 17.1 to 32.4 MPa for the F45-S, F75-S, F75-P, and F75-M mixes, respectively. The residual bond strength of each concrete mixture after being exposed to different high temperatures are compared, as shown in Fig. 7.

As can be seen from Fig. 7, the residual bond strength of each concrete mixture varied with the increasing temperature. At temperature of 400°C, the residual bond strength of the F75-M mix increased without attenuation. Moreover, at temperature of 600°C, the residual bond strength of the N45, F75-S, and F75-P mixes also increased without attenuation (compared to 400°C). As can be seen from Table 6, the residual strength ratio of these specimens

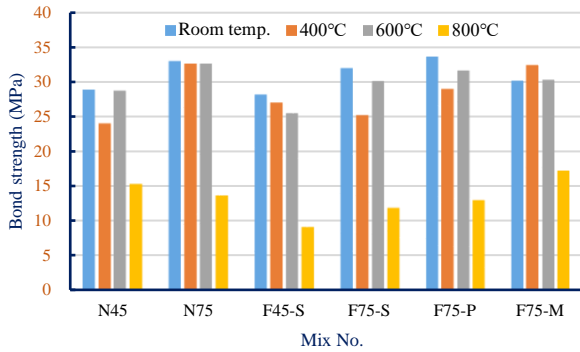
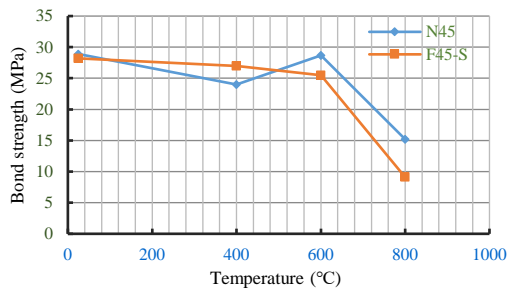
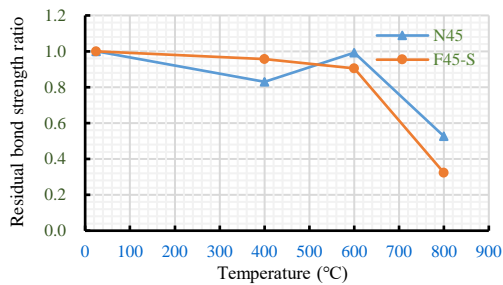


Fig. 7 Comparison of bond strength for concrete mixes



(a) Residual bond strength



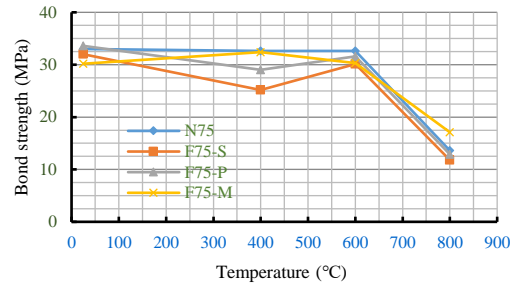
(b) Residual bond strength ratio

Fig. 8 Comparison of bond strength for medium strength concrete mixes

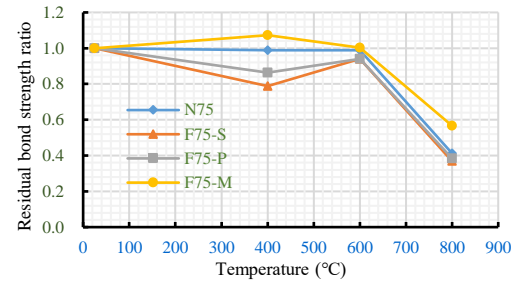
was about 0.94 to 1.07 after fire. However, once the temperature was raised to 800°C, the residual bond strength of each concrete mixture significantly decreased, and the residual strength ratios were lower than 0.57.

Fig. 8(a) shows that for the medium strength concrete, the bond strength of the experimental group decreased with the increasing temperature. However, the bond strength of the control group was more complicated with the increasing temperature. It reduced at 400°C, then increased at 600°C, but decreased again at 800°C. In addition, it can be seen from Fig. 8(b) that the trend of residual bond strength ratio in the control group and the experimental group was similar to that in Fig. 8(a).

As for the high strength concrete, however, it can be seen from Fig. 9(a) that the residual bond strengths of the F75-S and F75-P mixes in the experimental group were more complicated with the increasing temperature; while the trend of residual bond strength of the F75-M mix was more moderate with the increasing temperature. Moreover, it can also be seen from Fig. 9(b) that at temperature of



(a) Residual bond strength



(b) Residual bond strength ratio

Fig. 9 Comparison of bond strength for high strength concrete mixes

400°C, the residual bond strength ratio of the F75-M mix was the largest. The reason may be due to the increased tensile strength of steel fibers to resist thermal stress. In addition, when the internal temperature of the concrete reached about 170°C, the polypropylene fibers melted and provided micro channels to reduce the vapor pressure within the concrete. Therefore, F75-M can exhibit a better residual bond strength ratio. When the temperature was over 600°C, there was not much different in terms of residual bond strength ratio between the experimental group and the control group. From this perspective, the addition of fiber on the residual bond strength of concrete after exposure to elevated temperatures was not significant. However, after exposure to 400, 600, and 800°C, the high strength concrete with hybrid fiber retained, respectively, 107%, 100% and 57% of their bond strength, which were better than that for the concrete with individual fiber and the control concrete. This demonstrated that the use of hybrid combinations of steel fiber and polypropylene fiber can enhance the residual bond strength ratio of high strength concrete.

#### 4. Conclusions

In this study, steel fiber and polypropylene fiber were used to investigate the effects of individual and hybrid fiber on the local bond stress-slip relationship of medium and high strength concrete after exposure to elevated temperatures. On the basis of the above experimental results and discussion, the following conclusions were drawn:

- With the increase of concrete strength, the ultimate bond stress in the local bond stress versus slip curve of the high strength fiber reinforced concrete was higher than that

of the medium strength fiber reinforced concrete.

- At temperature of 400°C, the ascending slope of the local bond stress versus slip curve of the control group (N75) specimen was obviously attenuated, while the ascending slope of the F75-S and F75-M specimens in the experimental group was only slightly attenuated.

- At different temperatures, the slip of the ultimate bond stress of the N75 specimen in the control group of high strength concrete was quite large (except 800°C), and its value was about 25-27 mm. In contrast, the slip of the experimental group at 800 °C was relatively small, which was about 6-11 mm.

- At temperature of 400°C, the residual bond strength of the F75-M mix increased without attenuation. Moreover, at temperature of 600°C, the residual bond strength of the N45, F75-S, and F75-P mixes also increased without attenuation (compared to 400°C).

- At temperature of 800°C, the residual bond strength of each concrete mixture significantly decreased, and the residual strength ratios were lower than 0.57.

- After exposure to 400, 600, and 800°C, the high strength concrete with hybrid fiber retained, respectively, 107%, 100% and 57% of their bond strength, which were better than that for the concrete with individual fiber and the control concrete. This demonstrated that the use of hybrid combinations of steel fiber and polypropylene fiber can enhance the residual bond strength ratio of high strength concrete.

## Acknowledgments

This work was supported by the Ministry of Science and Technology (MOST), Taiwan. The author expresses his gratitude and sincere appreciation to MOST for financing this research work.

## References

- ACI-318 (1999), *Building Code Requirements for Reinforced Concrete and Commentary*, American Concrete Institute, Farmington Hills, Michigan, U.S.A.
- ACI-318 (2014), *Building Code Requirements for Reinforced Concrete and Commentary*, American Concrete Institute, Farmington Hills, Michigan, U.S.A.
- ACI Committee 408 (2003), *Bond and Development of Straight Reinforcing Bars in Tension (ACI 408R-03)*, American Concrete Institute, Farmington Hills, Michigan, U.S.A.
- Alexandre Bogas, J., Gomes, M.G. and Real, S. (2014), "Bonding of steel reinforcement in structural expanded clay lightweight aggregate concrete: The influence of failure mechanism and concrete composition", *Constr. Build. Mater.*, **65**, 350-359.
- ASTM C150/C150M-15 (2015), *Standard Specification for Portland Cement*, ASTM International, West Conshohocken, Pennsylvania, U.S.A.
- ASTM C33/C33M-13 (2013), *Standard Specification for Concrete Aggregates*, ASTM International, West Conshohocken, Pennsylvania, U.S.A.
- Bilodeau, A., Kodur, V.K.R. and Hoff, G.C. (2004), "Optimization of the type and amount of polypropylene fibres for preventing the spalling of lightweight concrete subjected to hydrocarbon fire", *Cement Concrete Compos.*, **26**(2), 163-174.
- Chan, Y.N, Luo, X. and Sun, W. (2000), "Compressive strength and pore structure of high-performance concrete after exposure to high temperature up to 800°C", *Cement Concrete Res.*, **30**(2), 247-251.
- Choi, J.I. and Lee, B.Y. (2015), "Bonding properties of basalt fiber and strength reduction according to fiber orientation", *Mater.*, **8**(10), 6719-6727.
- Dehestani, M. and Mousavi, S.S. (2015), "Modified steel bar model incorporating bond-slip effects for embedded element method", *Constr. Build. Mater.*, **81**, 284-290.
- Deng, Z.C., Jumbe, R.D. and Yuan, C.X. (2014), "Bonding between high strength rebar and reactive powder concrete", *Comput. Concrete*, **13**(3), 411-421.
- Ding, Y., Azevedo, C., Aguiar, J.B. and Jalali, S. (2012), "Study on residual behaviour and flexural toughness of fibre cocktail reinforced self compacting high performance concrete after exposure to high temperature", *Constr. Build. Mater.*, **26**(1), 21-31.
- Ergün, A., Kürklü, G. and Başpınar, M.S. (2016), "The effects of material properties on bond strength between reinforcing bar and concrete exposed to high temperature", *Constr. Build. Mater.*, **112**, 691-698.
- FIP/CEB (1990), *High Strength Concrete: State of the Art Report*, Bulletin d'Information No. 197. London, U.K.
- Golafshani, E.M., Rahai, A. and Kebria, S.S.H. (2014b), "Prediction of the bond strength of ribbed steel bars in concrete based on genetic programming", *Comput. Concrete*, **14**(3), 327-359.
- Golafshani, E.M., Rahai, A. and Sebt, M.H. (2014a), "Bond behavior of steel and GFRP bars in self-compacting concrete", *Constr. Build. Mater.*, **61**, 230-240.
- Golafshani, E.M., Rahai, A. and Sebt, M.H. (2015), "Artificial neural network and genetic programming for predicting the bond strength of GFRP bars in concrete", *Mater. Struct.*, **48**(5), 1581-1602.
- Golafshani, E.M., Rahai, A., Sebt, M.H. and Akbarpour, H. (2012), "Prediction of bond strength of spliced steel bars in concrete using artificial neural network and fuzzy logic", *Constr. Build. Mater.*, **36**, 411-418.
- Kim, M.J., Kim, S., Lee, S.K., Kim, J.H., Lee, K. and Yoo, D.Y. (2017), "Mechanical properties of ultra-high-performance fiber-reinforced concrete at cryogenic temperatures", *Constr. Build. Mater.*, **157**, 498-508.
- Kim, N.W., Lee, H.H. and Kim, C.H. (2016), "Fracture behavior of hybrid fiber reinforced concrete according to the evaluation of crack resistance and thermal", *Comput. Concrete*, **18**(5), 685-696.
- Ko, J., Ryu, D. and Noguchi, T. (2011), "The spalling mechanism of high-strength concrete under fire", *Mag. Concrete Res.*, **63**(5), 357-370.
- Kodur, V. (2014), *Properties of Concrete at Elevated Temperatures*, ISRN Civil Engineering Volume, Article ID 468510.
- Lee, H.H. and Yi, S.T. (2016), "Structural performance evaluation of steel fiber reinforced concrete beams with recycled aggregates", *Comput. Concrete*, **18**(5), 741-756.
- Mehta, P.K. and Monteiro, P.J.M. (2006), *Concrete: Microstructure, Properties, and Materials*, 3rd Edition, The McGraw-Hill Companies, Inc., New York, U.S.A.
- Mo, K.H., Alengaram, U.J., Visintin, P., Goh, S.H. and Jumaat, M.Z. (2015), "Influence of lightweight aggregate on the bond properties of concrete with various strength grades", *Constr. Build. Mater.*, **84**, 377-386.
- Nematzadeh, M. and Poorhosein, R. (2017), "Estimating properties of reactive powder concrete containing hybrid fibers using UPV", *Comput. Concrete*, **20**(4), 4915-4502.
- Ozawa, M. and Morimoto, M. (2014), "Effects of various fibres on

- high-temperature spalling in high-performance concrete”, *Constr. Build. Mater.*, **71**, 83-92.
- Poon, C.S., Shui, Z.H. and Lam, L. (2004), “Compressive behavior of fiber reinforced high-performance concrete subjected to elevated temperatures”, *Cement Concrete Res.*, **34**(12), 2215-2222.
- RILEM (1994), *Technical Recommendations for the Testing and Use of Construction Materials*, E&FN Spon, London, U.K.
- Ruano, G., Isla, F., Luccioni, B., Zerbino, R. and Giaccio, G. (2018), “Steel fibers pull-out after exposure to high temperatures and its contribution to the residual mechanical behavior of high strength concrete”, *Constr. Build. Mater.*, **163**, 571-585.
- Saleem, M. (2017), “Study to detect bond degradation in reinforced concrete beams using ultrasonic pulse velocity test method”, *Struct. Eng. Mech.*, **64**(4), 427-436.
- Siddique, R. and Kaur, D. (2012), “Properties of concrete containing ground granulated blast furnace slag (GGBFS) at elevated temperatures”, *J. Adv. Res.*, **3**(1), 45-51.
- Soroushian, P., Mirza, F. and Alhozaimy, A. (1994), “Bonding of confined steel fiber reinforced concrete to deformed bars”, *ACI Mater. J.*, **91**(2), 144-149.
- Tang, C.W. (2015), “Local bond stress-slip behavior of reinforcing bars embedded in lightweight aggregate concrete”, *Comput. Concrete*, **16**(3), 449-466.
- Tang, C.W. (2017), “Uniaxial bond stress-slip behavior of reinforcing bars embedded in lightweight aggregate concrete”, *Struct. Eng. Mech.*, **62**(5), 651-661.
- Varona, F.B., Baeza, F.J., Bru, D. and Ivorra, S. (2018), “Influence of high temperature on the mechanical properties of hybrid fibre reinforced normal and high strength concrete”, *Constr. Build. Mater.*, **159**, 73-82.
- Xiong, M.X. and Richard Liew, J.Y. (2015), “Spalling behavior and residual resistance of fibre reinforced ultra-high performance concrete after exposure to high temperatures”, *Mater. Constr.*, **65**(320), e071.
- Xu, M., Hallinan, B. and Wille, K. (2016), “Effect of loading rates on pullout behavior of high strength steel fibers embedded in ultra-high performance concrete”, *Cement Concrete Compos.*, **70**, 98-109.
- Yan, Z., Shen, Y., Zhu, H., Li, X. and Lu, Y. (2015), “Experimental investigation of reinforced concrete and hybrid fibre reinforced concrete shield tunnel segments subjected to elevated temperature”, *Fire Safety J.*, **71**, 86-99.
- Zhang, H. and Yu, R.C. (2016), “Inclined fiber pullout from a cementitious matrix: A numerical study”, *Mater.*, **9**(10), 800.
- Zhou, X., Mou, T., Tang, H. and Fan, B. (2017), “Experimental study on ultrahigh strength concrete filled steel tube short columns under axial load”, *Adv. Mater. Sci. Eng.*, **9**.